Hindawi Publishing Corporation
Differential Equations and Nonlinear Mechanics
Volume 2009, Article ID 842656, 26 pages
doi:10.1155/2009/842656

Research Article

Oscillation Susceptibility Analysis of the ADMIRE Aircraft along the Path of Longitudinal Flight Equilibriums in Two Different Mathematical Models

Stefan Balint,[1] Agneta Maria Balint,[2] and Achim Ionita[3]

[1] *Faculty of Mathematics and Computer Science, West University of Timisoara, Bulv. V.Parvan 4, 300223 Timisoara, Romania*
[2] *Faculty of Physics, West University of Timisoara, Bulv. V.Parvan 4, 300223 Timisoara, Romania*
[3] *Institute for Theoretical and Experimental Analysis of Aeronautical Structures, STRAERO, Bd.Iuliu Maniu 220, 061126, Bucharest, Romania*

Correspondence should be addressed to Agneta Maria Balint, balint@physics.uvt.ro

Received 8 March 2009; Revised 3 May 2009; Accepted 28 June 2009

Recommended by Nicola Bellomo

The oscillation susceptibility of the ADMIRE aircraft along the path of longitudinal flight equilibriums is analyzed numerically in the general and in a simplified flight model. More precisely, the longitudinal flight equilibriums, the stability of these equilibriums, and the existence of bifurcations along the path of these equilibriums are researched in both models. Maneuvers and appropriate piloting tasks for the touch-down moment are simulated in both models. The computed results obtained in the models are compared in order to see if the movement concerning the landing phase computed in the simplified model is similar to that computed in the general model. The similarity we find is not a proof of the structural stability of the simplified system, what as far we know never been made, but can increase the confidence that the simplified system correctly describes the real phenomenon.

1. Introduction

Frequently, we describe the evolution of real phenomena by systems of ordinary differential equations. These systems express physical laws and geometrical connections, and often they are obtained by neglecting some influences and quantities, which are assumed insignificant with respect to the others. If the obtained simplified system correctly describes the real phenomenon, then it has to be topologically equivalent to the system in which the small influences and quantities (which have been neglected) are also included. Furthermore, the simplified system has to be structurally stable. Therefore, when a simplified model of a real phenomenon is build up, it is desirable to verify the structural stability of the system.

Interest in oscillation susceptibility of an aircraft is generated by crashes of high-performance fighter airplanes, such as the YF-22A and B-2, due to the oscillations that were not predicted during the aircraft development [1]. Flying qualities and oscillation prediction are based on linear methods and their quasilinear extensions [2]. These analyses cannot, in general, predict the presence or the absence of oscillations, because of the large variety of nonlinear interactions that have been identified as factors contributing to oscillations. Some of these factors include pilot behavioral transitions, actuator rate limiting [3–5], and changes in aircraft dynamics caused by transitions in operating conditions [6], gain scheduling, and switching [7]. The oscillation susceptibility analysis in a nonlinear model involves the computation of nonlinear phenomena including bifurcations (Hopf or fold bifurcations) that leads sometimes to large changes in the stability of the aircraft.

Oscillation susceptibility analysis means the evaluation of the oscillation potential of a given aircraft: identify characteristics of the pilot-aircraft interaction that may result in oscillation, demonstrate the potential for oscillation by analysis and simulations using appropriate piloting tasks and test maneuvers, distinguish aircraft configurations that are less susceptible to oscillations from those that have high oscillations potential, and suggest to reduce and/or eliminate oscillation susceptibility [1].

As an example in [1] the X-15 aircraft oscillation caused by the rate limiting and an F/A-18 aircraft oscillation caused by nonlinear category III triggers are presented. The limit cycle amplitudes are computed for the longitudinal flight equations of motion and large jump in limit cycle amplitude indicating a significant change in the vehicle stability is revealed.

Our aim in this paper is to analyze numerically the oscillation susceptibility of the ADMIRE aircraft in a longitudinal flight in a quasilinear (simplified) and a nonlinear (general) flight model in landing phase, when the Automatic flight Control System (AFCS) is decoupled. The equations governing such a flight and the conditions which assure the existence of such a flight are presented. The equilibriums flights are analyzed numerically, from the point of view of bifurcations which can appear due to the changes of the elevator deflection. Appropriate piloting tasks and maneuvers for the touch-down moment are established. The behavior of the aircraft is simulated in both models. The computed results obtained in the models are compared in order to see if the simplified model correctly describes the real flight. This is not a proof of the structural stability of the simplified system but can increase the trust that the simplified system correctly describes the real phenomenon.

2. The General Nonlinear Model

The system of differential equations [8, 9], which describes the motion around the center of gravity of a rigid aircraft, with respect to an xyz body-axis system, where xz is the plane of symmetry, is

$$\frac{\overset{\circ}{V}}{V} \cdot \cos\alpha \cdot \cos\beta - \overset{\circ}{\beta} \cdot \cos\alpha \cdot \sin\beta - \overset{\circ}{\alpha} \cdot \sin\alpha \cdot \cos\beta$$

$$= r \cdot \sin\beta - q \cdot \sin\alpha \cdot \cos\beta - \frac{g}{V} \cdot \sin\theta + \frac{X}{m \cdot V},$$

$$\frac{\overset{\circ}{V}}{V} \cdot \sin\beta + \overset{\circ}{\beta} \cdot \cos\beta = p \cdot \sin\alpha \cdot \cos\beta - r \cdot \cos\alpha \cdot \cos\beta + \frac{g}{V} \cdot \sin\varphi \cdot \cos\theta + \frac{Y}{m \cdot V},$$

$$\begin{aligned}
&\frac{\overset{\circ}{V}}{V} \cdot \sin\alpha \cdot \cos\beta - \overset{\circ}{\beta} \cdot \sin\alpha \cdot \sin\beta + \overset{\circ}{\alpha} \cdot \cos\alpha \cdot \cos\beta \\
&\qquad = -p \cdot \sin\beta + q \cdot \cos\alpha \cdot \cos\beta + \frac{g}{V} \cdot \cos\varphi \cdot \cos\theta + \frac{Z}{m \cdot V}, \\
&I_x \cdot \overset{\circ}{p} - I_{xz} \cdot \overset{\circ}{r} = \left(I_y - I_z\right) \cdot q \cdot r + I_{xz} \cdot p \cdot q + L, \\
&I_y \cdot \overset{\circ}{q} = (I_z - I_x) \cdot p \cdot r - I_{xz} \cdot \left(p^2 - r^2\right) + M, \\
&I_z \cdot \overset{\circ}{r} - I_{xz} \cdot \overset{\circ}{p} = \left(I_x - I_y\right) \cdot p \cdot q - I_{xz} \cdot q \cdot r + N, \\
&\overset{\circ}{\varphi} = p + q \cdot \sin\varphi \cdot \tan\theta + r \cdot \cos\varphi \cdot \tan\theta, \\
&\overset{\circ}{\theta} = q \cdot \cos\varphi - r \cdot \sin\varphi, \\
&\overset{\circ}{\psi} = \frac{q \cdot \sin\varphi + r \cdot \cos\varphi}{\cos\theta}.
\end{aligned} \tag{2.1}$$

The state parameters of this system are forward velocity V, angle of attack α, sideslip angle β, roll rate p, pitch rate q, yaw rate r, Euler roll angle φ, Euler pitch angle θ, and Euler yaw angle ψ. The constants I_x, I_y, and I_z are the moments of inertia about the x-, y-, and z-axis, respectively, I_{xz} is the product of inertia, g is the gravitational acceleration, and m is the mass of the vehicle. The aero dynamical forces X, Y, Z and moments L, M, N are functions of the state parameters and the control parameters: δ_a is the aileron deflection, δ_e is the elevator deflection, and δ_r is the rudder deflection (the body flap, speed break, δ_c, δ_{ca} are available as additional controls but, for simplicity, they are set to 0 in the analysis to follow).

Definition 2.1. A flight with constant forward velocity V is defined as a flight for which $V =$ const (i.e., $\overset{\circ}{V} = 0$).

Proposition 2.2. *In a flight with constant forward velocity V the following equalities hold:*

$$\begin{aligned}
-\overset{\circ}{\beta} \cdot \cos\alpha \cdot \sin\beta - \overset{\circ}{\alpha} \cdot \sin\alpha \cdot \cos\beta &= r \cdot \sin\beta - q \cdot \sin\alpha \cdot \cos\beta - \frac{g}{V} \cdot \sin\theta + \frac{X}{m \cdot V}, \\
\overset{\circ}{\beta} \cdot \cos\beta &= p \cdot \sin\alpha \cdot \cos\beta - r \cdot \cos\alpha \cdot \cos\beta + \frac{g}{V} \cdot \sin\varphi \cdot \cos\theta + \frac{Y}{m \cdot V}, \\
-\overset{\circ}{\beta} \cdot \sin\alpha \cdot \sin\beta + \overset{\circ}{\alpha} \cdot \cos\alpha \cdot \cos\beta &= -p \cdot \sin\beta + q \cdot \cos\alpha \cdot \cos\beta + \frac{g}{V} \cdot \cos\varphi \cdot \cos\theta + \frac{Z}{m \cdot V},
\end{aligned} \tag{2.2}$$

Proof. Replacing $\overset{\circ}{V}$ by 0 in the system (2.1), then (2.2) is obtained. □

Proposition 2.3. *If in a flight with constant forward velocity V one has $\beta \equiv (2n+1)\cdot \pi/2$, then the following equalities hold:*

$$
\begin{gathered}
(-1)^n \cdot r - \frac{g}{V}\cdot \sin\theta + \frac{X}{m\cdot V} \equiv 0,\\
\frac{g}{V}\cdot \sin\varphi \cdot \cos\theta + \frac{Y}{m\cdot V} \equiv 0,\\
(-1)^{n+1}\cdot p + \frac{g}{V}\cdot \cos\varphi\cdot\cos\theta + \frac{Z}{m\cdot V} \equiv 0.
\end{gathered}
\tag{2.3}
$$

Proof. Replacing $\overset{\circ}{\beta} = 0$ and $\beta \equiv (2n+1)\cdot\pi/2$ in (2.2), then (2.3) is obtained. □

Proposition 2.4. *If in a flight with constant forward velocity V one has $\beta \neq (2n+1)\cdot\pi/2$, then the following equality holds:*

$$
\begin{aligned}
&g\left[\sin\beta\cdot\sin\varphi\cdot\cos\theta - \cos\alpha\cdot\cos\beta\cdot\sin\theta + \sin\alpha\cdot\cos\beta\cdot\cos\varphi\cdot\cos\theta\right]\\
&\quad + \frac{Y}{m}\cdot\sin\beta + \frac{X}{m}\cdot\cos\alpha\cdot\cos\beta + \frac{Z}{m}\cdot\sin\alpha\cdot\cos\beta \equiv 0.
\end{aligned}
\tag{2.4}
$$

Proof. Equation (2.4) is the solvability (compatibility) condition of system (2.2) when $\beta \neq (2n+1)\cdot\pi/2$. □

Proposition 2.5. *If $\beta \neq (2n+1)\cdot\pi/2$ and equality* (2.4) *holds, then the system* (2.2) *can be solved with respect to $\overset{\circ}{\alpha}$, $\overset{\circ}{\beta}$, obtaining the explicit system of differential equations, which describes the motion of the aircraft in a flight, with constant forward velocity V:*

$$
\begin{aligned}
\overset{\circ}{\alpha} &= q - p\cdot\cos\alpha\cdot\tan\beta - r\cdot\sin\alpha\cdot\tan\beta + \frac{g}{V\cdot\cos\beta}\cdot\left[\cos\varphi\cdot\cos\theta\cdot\cos\alpha + \sin\theta\cdot\sin\alpha\right]\\
&\quad + \frac{1}{\cos\beta}\cdot\left[\frac{Z}{m\cdot V}\cdot\cos\alpha - \frac{X}{m\cdot V}\cdot\sin\alpha\right],\\
\overset{\circ}{\beta} &= p\cdot\sin\alpha - r\cdot\cos\alpha + \frac{1}{\cos\beta}\cdot\frac{g}{V}\cdot\sin\varphi\cdot\cos\theta + \frac{1}{\cos\beta}\cdot\frac{Y}{m\cdot V},\\
I_x\cdot\overset{\circ}{p} - I_{xz}\cdot\overset{\circ}{r} &= \left(I_y - I_z\right)\cdot q\cdot r + I_{xz}\cdot p\cdot q + L,\\
I_y\cdot\overset{\circ}{q} &= (I_z - I_x)\cdot p\cdot r - I_{xz}\cdot\left(p^2 - r^2\right) + M,\\
I_z\cdot\overset{\circ}{r} - I_{xz}\cdot\overset{\circ}{p} &= \left(I_x - I_y\right)\cdot p\cdot q - I_{xz}\cdot q\cdot r + N,\\
\overset{\circ}{\varphi} &= p + q\cdot\sin\varphi\cdot\tan\theta + r\cdot\cos\varphi\cdot\tan\theta,\\
\overset{\circ}{\theta} &= q\cdot\cos\varphi - r\cdot\sin\varphi,\\
\overset{\circ}{\psi} &= \frac{q\cdot\sin\varphi + r\cdot\cos\varphi}{\cos\theta}.
\end{aligned}
\tag{2.5}
$$

Proof. System (2.5) is obtained solving system (2.2) with respect to $\overset{\circ}{\alpha}$, $\overset{\circ}{\beta}$ and replacing in system (2.1), then $(2.1)_1$, $(2.1)_2$, and $(2.1)_3$ with the above obtained $\overset{\circ}{\alpha}$ and $\overset{\circ}{\beta}$. □

Definition 2.6. A longitudinal flight is defined as a flight for which

$$\beta \equiv p \equiv r \equiv \varphi \equiv \psi \equiv 0, \qquad \delta_a = \delta_r = 0. \tag{2.6}$$

Proposition 2.7. *A longitudinal flight is possible if and only if* $Y = L = N = 0$ *for* $\beta = p = r = \varphi = \psi = 0$ *and* $\delta_a = \delta_r = 0$.

Proof. This result is obtained from (2.1) taking into account Definition 2.6. □

Proposition 2.8. *The explicit system of differential equations which describes the motion of the aircraft in a longitudinal flight is*

$$\begin{gathered}
\overset{\circ}{V} = g \cdot \sin(\alpha - \theta) + \frac{X}{m} \cdot \cos\alpha + \frac{Z}{m} \cdot \sin\alpha, \\
\overset{\circ}{\alpha} = q + \frac{g}{V} \cdot \cos(\theta - \alpha) - \frac{X}{m \cdot V} \cdot \sin\alpha + \frac{Z}{m \cdot V} \cdot \cos\alpha, \\
\overset{\circ}{q} = \frac{M}{I_y}, \\
\overset{\circ}{\theta} = q.
\end{gathered} \tag{2.7}$$

Proof. This result is obtained from (2.1) taking into account Definition 2.6. □

Remark 2.9. In system (2.7) X, Z, M depend only on α, q, θ, and δ_e. These dependences are obtained replacing in the general expression of the aerodynamic forces and moments: $\beta = p = r = \varphi = \psi = 0$ and $\delta_a = \delta_r = 0$.

Proposition 2.10. *The explicit system of differential equations which describes the motion of the aircraft in a longitudinal flight with constant forward velocity* V *is*

$$\begin{gathered}
\overset{\circ}{\alpha} = q + \frac{g}{V} \cdot \cos(\theta - \alpha) - \frac{X}{m \cdot V} \cdot \sin\alpha + \frac{Z}{m \cdot V} \cdot \cos\alpha, \\
\overset{\circ}{q} = \frac{M}{I_y}, \\
\overset{\circ}{\theta} = q.
\end{gathered} \tag{2.8}$$

Proof. This system is obtained from (2.7) taking into account $\overset{\circ}{V} = 0$. □

Proposition 2.11. *A longitudinal flight with constant forward velocity is possible if the following equalities hold:*

$$Y = L = N = 0 \quad \text{for } \beta = p = r = \varphi = \psi = 0, \qquad \delta_a = \delta_r = 0, \tag{2.9}$$

$$g \cdot \sin(\alpha - \theta) + \frac{X}{m} \cdot \cos\alpha + \frac{Z}{m} \cdot \sin\alpha = 0. \tag{2.10}$$

Proof. This result is obtained from Proposition 2.7 and system (2.7), taking into account the fact that $\overset{\circ}{V}$ is equal to zero. □

Remark 2.12. Notice that in (2.8) and (2.10) X, Z, M depend on α, q, θ, δ_e, and V. Taking into account (2.10), the system (2.8) can be written as

$$\begin{gathered}
\overset{\circ}{\alpha} = q + \frac{g}{V} \cdot \cos(\theta - \alpha) - \frac{g}{V} \cdot \sin(\theta - \alpha) \cdot \tan\alpha + \frac{Z}{m \cdot V} \cdot \frac{1}{\cos\alpha}, \\
\overset{\circ}{q} = \frac{M}{I_y}, \\
\overset{\circ}{\theta} = q.
\end{gathered} \tag{2.11}$$

Remark 2.13. In system (2.11), the functions $Z = Z(\alpha, q, \theta;\ \delta_e, V)$ and $M = M(\alpha, q, \theta;\ \delta_e, V)$ are considered known; δ_e and V are parameters.

The system (2.11) describes the motion around the center of gravity of an aircraft in a longitudinal flight with constant forward velocity V and defines the general nonlinear model.

3. The Simplified Model of the ADMIRE Aircraft

The ADMIRE aircraft is an Aero Data Model In a Research Environment. To describe the flight of this vehicle with constant forward velocity V, the following explicit system of differential equations is employed:

$$\begin{aligned}
\overset{\circ}{\alpha} &= q - p \cdot \beta + \frac{g}{V} \cdot \cos\theta \cdot \cos\varphi + z_\alpha \cdot \alpha + y_\beta \cdot \beta^2 + y_p(\alpha, \beta) \cdot p \cdot \beta + y_r(\beta) \cdot r \cdot \beta \\
&\quad + y_{\delta_a} \cdot \beta \cdot \delta_a + z_{\delta_e} \cdot \delta_e + y_{\delta_r} \cdot \beta \cdot \delta_r, \\
\overset{\circ}{\beta} &= p \cdot\ \alpha - r + \frac{g}{V} \cdot \sin\varphi \cdot \cos\theta - z_\alpha \cdot \alpha \cdot \beta + y_\beta \cdot \beta - y_p(\alpha, \beta) \cdot p - y_r(\beta) \cdot r \\
&\quad + y_{\delta_a} \cdot \delta_a - z_{\delta_e} \cdot \beta \cdot \delta_e + y_{\delta_r} \cdot \delta_r, \\
\overset{\circ}{p} &= -i_1 \cdot q \cdot r + l_\beta(\alpha) \cdot \beta + l_p \cdot p + l_r(\alpha) \cdot r + l_{\delta_a} \cdot \delta_a + l_{\delta_r} \cdot \delta_r,
\end{aligned}$$

$$
\begin{aligned}
\overset{\circ}{q} &= i_2 \cdot p \cdot r + m_\alpha \cdot \alpha + m_q \cdot q - \overline{m_{\overset{\circ}{\alpha}}} \cdot p \cdot \beta + \overline{y_p} \cdot p \cdot \beta + \overline{y_\beta} \cdot \beta^2 + \overline{y_r}(\beta) \cdot r \cdot \beta \\
&\quad + \frac{g}{V} \cdot \left(\overline{m_{\overset{\circ}{\alpha}}} \cdot \cos\theta \cdot \cos\varphi - \frac{c_2}{a} \cdot a_2 \cdot \sin\theta \right) + \overline{y_{\delta_a}} \cdot \beta \cdot \delta_a + m_{\delta_c} \cdot \delta_c + m_{\delta_e} \cdot \delta_e + \overline{y_{\delta_r}} \cdot \beta \cdot \delta_r, \\
\overset{\circ}{r} &= -i_3 \cdot p \cdot q + n_\beta \cdot \beta + n_p(\alpha, \beta) \cdot p + n_r(\alpha, \beta) \cdot r + n_{\delta_a} \cdot \delta_a + n_{\delta_{ca}}(\alpha) \cdot \delta_{ca} + n_{\delta_r} \cdot \delta_r, \\
\overset{\circ}{\varphi} &= p + (q \cdot \sin\varphi + r \cdot \cos\varphi) \cdot \tan\theta, \\
\overset{\circ}{\theta} &= q \cdot \cos\varphi - r \cdot \sin\varphi, \\
\overset{\circ}{\psi} &= \frac{q \cdot \sin\varphi + r \cdot \cos\varphi}{\cos\theta}.
\end{aligned}
\tag{3.1}
$$

Proposition 3.1. *System* (3.1) *can be obtained from* (2.5) *substituting the general aero dynamical forces and moments with those corresponding to the ADMIRE aircraft [10], assuming that α and β are small and making the following approximations:*

$(2.5)_1$ $\cos\beta \approx 1$; $-p \cdot \cos\alpha \cdot \tan\beta \approx -p \cdot \beta$; $-r \cdot \sin\alpha \cdot \tan\beta \approx 0$; $\cos\alpha \approx 1$; $\sin\alpha \approx 0$,

$(2.5)_2$ $\cos\beta \approx 1$

$$
\begin{gathered}
\frac{I_{xz} \cdot (I_x + I_z - I_y)}{I_x \cdot I_z - I_{xz}^2} \approx 0, \qquad \frac{(I_y - I_z) \cdot I_z - I_{xz}^2}{I_x \cdot I_z - I_{xz}^2} \approx -i_1, \qquad \frac{I_{xz}}{I_y} \approx 0; \\
\frac{I_{xz}^2 + (I_x - I_y) \cdot I_x}{I_x \cdot I_z - I_{xz}^2} \approx -i_3, \qquad \frac{I_{xz} \cdot (I_y - I_z - I_{xz})}{I_x \cdot I_z - I_{xz}^2} \approx 0.
\end{gathered}
\tag{3.2}
$$

Proof. The proof is given by computation. □

Proposition 3.2. *The simplified system which governs the longitudinal flight with constant forward velocity V of the ADMIRE aircraft is*

$$
\begin{aligned}
\overset{\circ}{\alpha} &= q + \frac{g}{V} \cdot \cos\theta + z_\alpha \cdot \alpha + z_{\delta_e} \cdot \delta_e, \\
\overset{\circ}{q} &= m_\alpha \cdot \alpha + m_q \cdot q + \frac{g}{V} \cdot \left(\overline{m_{\overset{\circ}{\alpha}}} \cdot \cos\theta - \frac{c_2}{a} \cdot a_2 \cdot \sin\theta \right) + m_{\delta_e} \cdot \delta_e, \\
\overset{\circ}{\theta} &= q.
\end{aligned}
\tag{3.3}
$$

Proof. System (3.3) is obtained from the system (3.1) for $\beta = p = r = \varphi = 0$ and $\delta_a = \delta_r = \delta_c = \delta_{ca} = 0$ and defines the simplified nonlinear model of the motion around the center of gravity of the ADMIRE aircraft in a longitudinal flight with constant forward velocity V.

In system (3.3) g, V, z_α, z_{δ_e}, m_α, m_q, $\overline{m_{\overset{\circ}{\alpha}}}$, c_2, a_2, a, m_{δ_e} are considered constants (see Table 1). □

Remark 3.3. According to the simplified nonlinear model the equilibriums in a longitudinal flight with constant forward velocity are the solutions of the nonlinear system of equations:

$$\begin{gathered} q + \frac{g}{V} \cdot \cos\theta + z_\alpha \cdot \alpha + z_{\delta_e} \cdot \delta_e = 0, \\ m_\alpha \cdot \alpha + m_q \cdot q + \frac{g}{V} \cdot \left(\overline{m_{\overset{\circ}{\alpha}}} \cdot \cos\theta - \frac{c_2}{a} \cdot a_2 \cdot \sin\theta \right) + m_{\delta_e} \cdot \delta_e = 0, \\ q = 0. \end{gathered} \tag{3.4}$$

System (3.4) defines the equilibriums manifold of the longitudinal flight with constant forward velocity V.

Proposition 3.4. *System* (3.4) *implies that* α *satisfies*

$$A \cdot \alpha^2 + B \cdot \delta_e \cdot \alpha + C \cdot \delta_e^2 + D = 0, \tag{3.5}$$

where A, B, C, D *are given by*

$$\begin{aligned} A &= \left(m_\alpha - \overline{m_{\overset{\circ}{\alpha}}} \cdot z_\alpha \right)^2 + \frac{{c_2}^2}{a^2} \cdot {a_2}^2 \cdot {z_\alpha}^2, \\ B &= 2 \cdot \left(m_\alpha - \overline{m_{\overset{\circ}{\alpha}}} \cdot z_\alpha \right) \cdot \left(m_{\delta_e} - \overline{m_{\overset{\circ}{\alpha}}} \cdot z_{\delta_e} \right) + 2 \cdot \frac{{c_2}^2}{a^2} \cdot {a_2}^2 \cdot z_\alpha \cdot z_{\delta_e}, \\ C &= \left(m_{\delta_e} - \overline{m_{\overset{\circ}{\alpha}}} \cdot z_{\delta_e} \right)^2 + \frac{{c_2}^2}{a^2} \cdot {a_2}^2 \cdot {z_{\delta_e}}^2, \\ D &= -\frac{g^2}{V^2} \cdot \frac{{c_2}^2}{a^2} \cdot {a_2}^2. \end{aligned} \tag{3.6}$$

Proof. Equation (3.5) is obtained replacing $q = 0$ in $(3.4)_1$ and $(3.4)_2$ and eliminating θ between the so-obtained equations. □

For the numerical values given in Table 1, (3.5) has real solutions if and only if $\delta_e \in [\underline{\delta_e}, \overline{\delta_e}]$ where $\underline{\delta_e} = -0.04678233231992$ [rad] $= -2.681^\circ$ and $\overline{\delta_e} = -\underline{\delta_e}$.

The computed $\alpha_1(\delta_e)$, $\theta_1(\delta_e)$, $\alpha_2(\delta_e)$, and $\theta_2(\delta_e)$ solutions are represented on Figures 1 and 2.

The equilibrium manifold $\mathscr{M}_V$ is the union of the following two pieces:

$$\mathcal{P}_1 = \left\{ (\alpha_1(\delta_e), 0, \theta_1(\delta_e)) : \delta_e \in \left[\underline{\delta_e}, \overline{\delta_e}\right] \right\}, \qquad \mathcal{P}_2 = \left\{ (\alpha_2(\delta_e), 0, \theta_2(\delta_e)) : \delta_e \in \left[\underline{\delta_e}, \overline{\delta_e}\right] \right\}. \tag{3.7}$$

Table 1: The values of the parameters used in the simplified system (3.3).

Parameter	Value	Units
z_α	−1.598075	rad/s
z_{δ_e}	−0.52089	rad/s
m_α	1.72514652738	rad/s^2
m_q	−22.61196	rad/s^2
a	−0.485	s^{-1}
m_{δ_e}	−9.972922	—
a_2	11.964	s^{-2}
V	84.5	m/s
g	9.81	m/s^2
$\overline{m_{\dot\alpha}}$	−5.26416	rad/s^2
c_2	−0.029	—
—	—	—

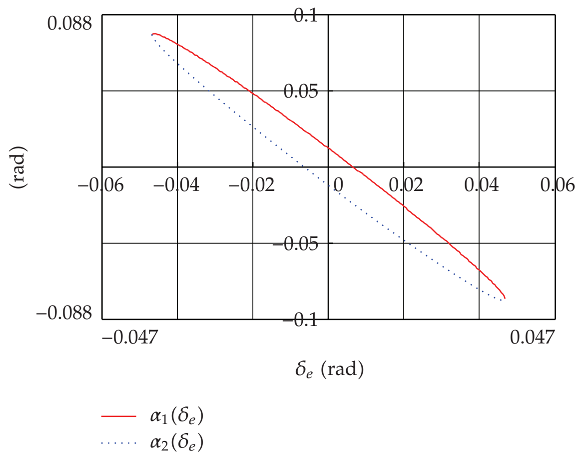

Figure 1: The $\alpha_1(\delta_e)$ and $\alpha_2(\delta_e)$ coordinates of the equilibriums on the manifold $\mathcal{M}_V$.

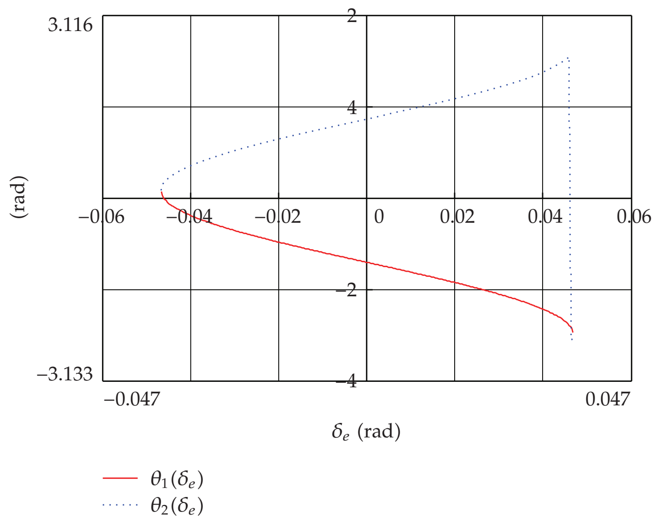

Figure 2: The $\theta_1(\delta_e) + 2k\pi$ and $\theta_2(\delta_e) + 2k\pi$ coordinates of the equilibriums on the manifold $\mathcal{M}_V$.

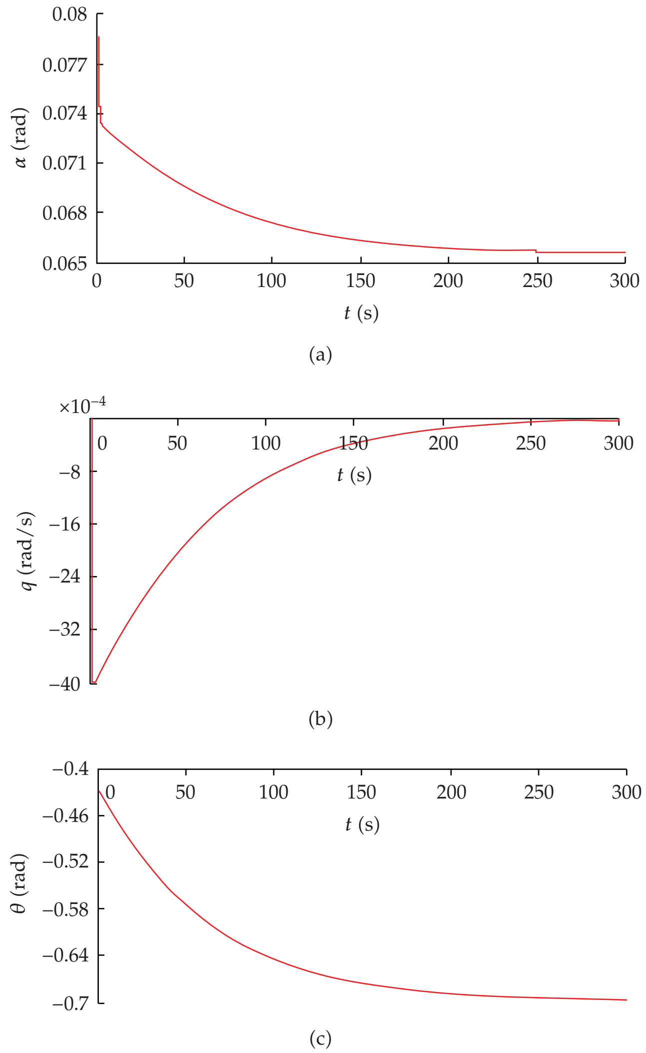

Figure 3: A transfer between two equilibriums, which belong to $\mathcal{D}_1$ (simulated in simplified model): $\delta'_e = -0.03866\,[\text{rad}] = 2.216^\circ \rightarrow \delta''_e = 0.03026\,[\text{rad}] = 1.734^\circ$. $\alpha'_1 = 0.07866974\,[\text{rad}] = 4.509^\circ$; $q'_1 = 0\,[\text{rad/s}]$; $\theta'_1 = -0.428832\,[\text{rad}] = 24.582^\circ \rightarrow \alpha''_1 = 0.065516\,[\text{rad}] = 3.755^\circ$; $q''_1 = 0\,[\text{rad/s}]$; $\theta''_1 = -\,0.698066\,[\text{rad}] = -40.016^\circ$.

Proposition 3.5. *The eigenvalues of the linearized system at an equilibrium are the solutions of the equation:*

$$-\lambda^3 + \left(z_\alpha + m_q\right) \cdot \lambda^2 + \left(m_\alpha + a_{23} - z_\alpha \cdot m_q\right) \cdot \lambda + m_\alpha \cdot \frac{g}{V} \cdot \sin\theta - z_\alpha \cdot a_{23} = 0, \tag{3.8}$$

where $a_{23} = -(g/V) \cdot [\overline{m_{\mathring{\alpha}}} \cdot \sin\theta - (c_2/a) \cdot a_2 \cdot \cos\theta]$.

Proof. The proof is given by computation. □

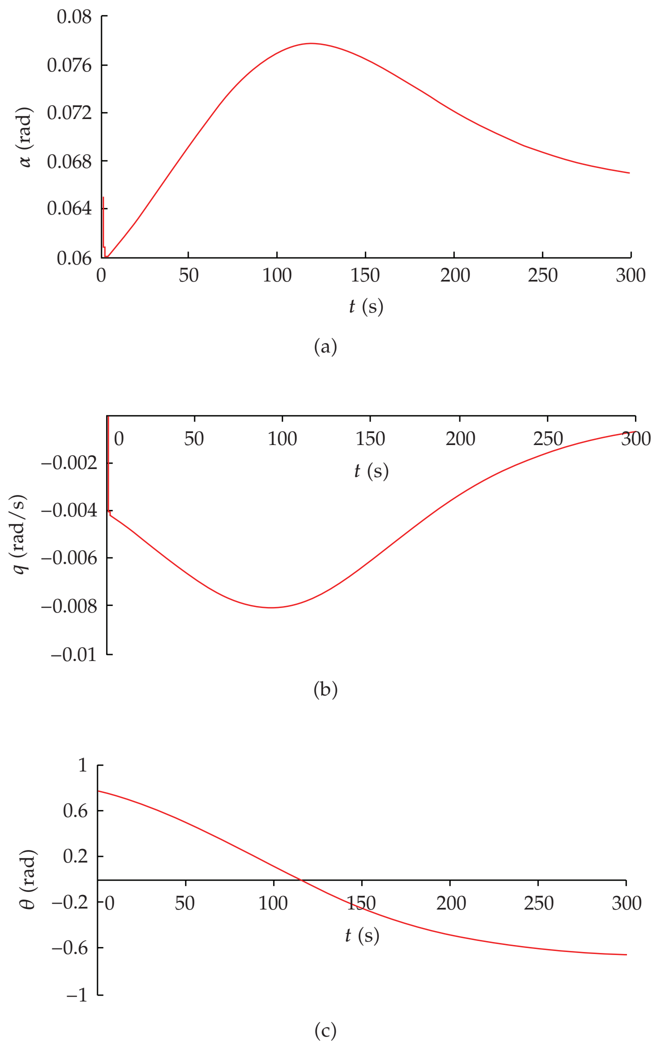

Figure 4: A transfer of an equilibrium, which belongs to $\mathcal{P}_2$ into an equilibrium, which belongs to $\mathcal{P}_1$ (simulated in the simplified model): $\delta_e' = -0.03866\,[\text{rad}] = 2.216^\circ \longrightarrow \delta_e'' = 0.03026\,[\text{rad}] = 1.734^\circ$. $\alpha_2' = 0.064883\,[\text{rad}] = 3.719^\circ$; $q_2' = 0\,[\text{rad/s}]$; $\theta_2' = 0.7674624\,[\text{rad}] = 43.994^\circ \longrightarrow \alpha_1'' = 0.065516\,[\text{rad}] = 3.755^\circ$; $q_1'' = 0\,[\text{rad/s}]$; $\theta_1'' = -0.6980667\,[\text{rad}] = -40.016^\circ$ instead of $\alpha_2' = 0.064883\,[\text{rad}] = 3.719^\circ$; $q_2' = 0\,[\text{rad/s}]$; $\theta_2' = 0.7674624\,[\text{rad}] = 43.994^\circ \longrightarrow \alpha_2'' = 0.046845\,[\text{rad}] = 2.685^\circ$; $q_2'' = 0\,[\text{rad/s}]$; $\theta_2'' = 1.03669718\,[\text{rad}] = 59.428^\circ$.

Proposition 3.6. *For $\delta_e \in (\underline{\delta_e}, \overline{\delta_e})$ the equilibriums of $\mathcal{P}_1$ are exponentially stable and those of $\mathcal{P}_2$ are unstable.*

Proof. These results were obtained computing the eigenvalues of the linearized system at the equilibriums of $\mathcal{P}_1$ and at the equilibriums of $\mathcal{P}_2$. More precisely, it was obtained that the eigenvalues are negative real numbers at the equilibriums of $\mathcal{P}_1$, and two of the eigenvalues are negative and the third is positive at the equilibriums of $\mathcal{P}_2$. □

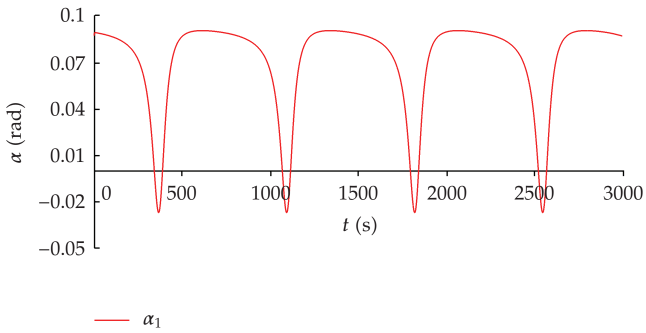

(a)

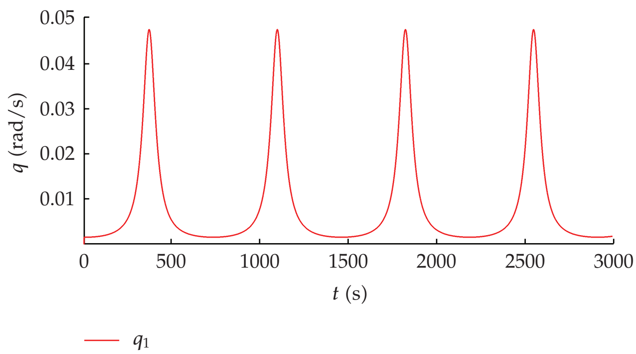

(b)

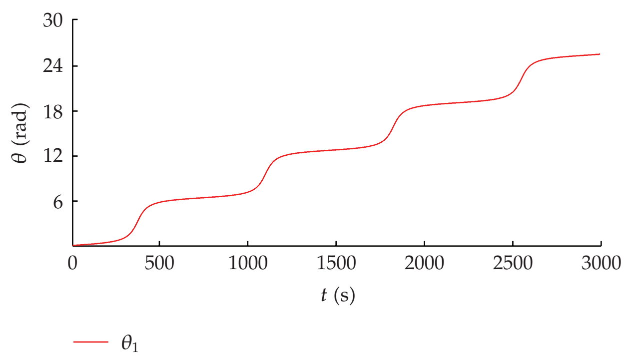

(c)

Figure 5: Oscillations when $\delta_e' = -0.04678\,[\mathrm{rad}] = -2.68^\circ \rightarrow \delta_e'' = -0.05\,[\mathrm{rad}] = -2.866^\circ$ and the starting point is $\alpha_1' = 0.0869742\,[\mathrm{rad}] = 4.985^\circ$; $q_1' = 0\,[\mathrm{rad/sec}]$; $\theta_1' = 0.159329\,[\mathrm{rad}] = 9.133^\circ$.

Proposition 3.7. *At the equilibriums, which correspond to $\underline{\delta_e}$ and $\overline{\delta_e}$, two of the eigenvalues are negative and one eigenvalue is equal to zero. Consequently, $\underline{\delta_e}$ and $\overline{\delta_e}$ are nonhyperbolic equilibrium points (turning points).*

Proof. The proof is given by computation. □

Remark 3.8. Transfers between two equilibriums which belong to a conex part of $\mathcal{P}_1 = \{(\alpha_1(\delta_e), 0, \theta_1(\delta_e)) : \delta_e \in (\underline{\delta_e}, \overline{\delta_e})\}$ are possible by small changes of the elevator deflection

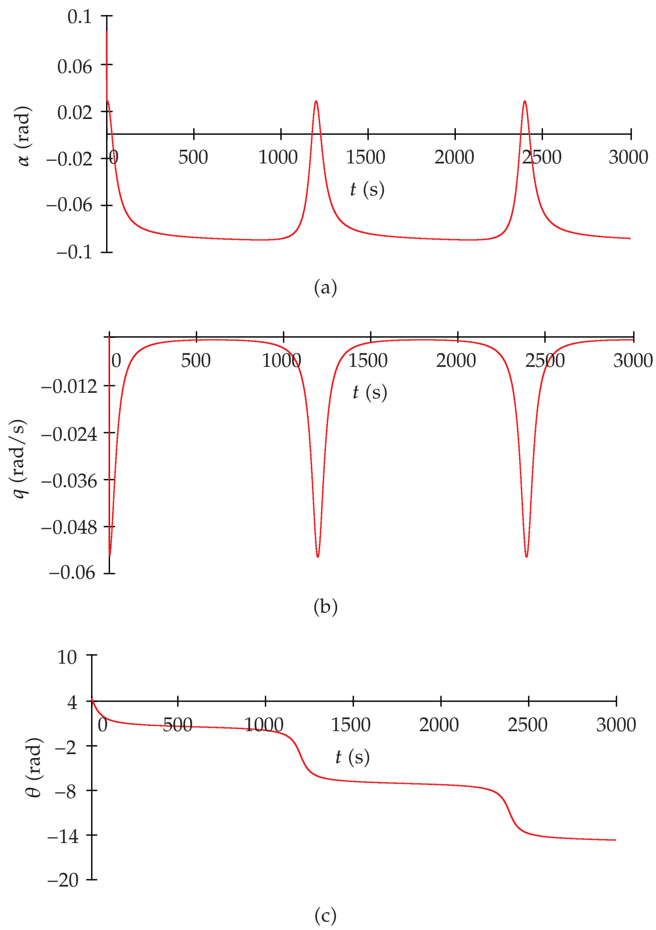

Figure 6: Oscillations when $\delta_e' = -0.04678$ [rad] $= -2.681°$ $\rightarrow$ $\delta_e'' = 0.048$ [rad] $= 2.751°$ and the starting point is $\alpha_1' = 0.086974288$ [rad] $= 4.985°$; $q_1' = 0$ [rad/sec]; $\theta_1' = 0.1593297$ [rad] $= 9.133°$.

δ_e (Figure 3). On the other hand, a small change of the elevator deflection δ_e transfers an equilibrium which belongs to $\wp_2 = \{(\alpha_2(\delta_e), 0, \theta_2(\delta_e)) : \delta_e \in (\underline{\delta_e}, \overline{\delta_e})\}$ into an equilibrium which belongs to $\wp_1$ (Figure 4).

Remark 3.9. The behavior of the ADMIRE aircraft changes when the maneuver $\delta_e' \rightarrow \delta_e''$ is so that $\delta_e' \in (\underline{\delta_e}, \overline{\delta_e})$ and $\delta_e'' \notin (\underline{\delta_e}, \overline{\delta_e})$. Computation shows that after such a maneuver α and q oscillate with the same period and θ tends to $+\infty$ or $-\infty$ (Figures 5 and 6).

Since the nonhyperbolic equilibriums at $\underline{\delta_e}$ and $\overline{\delta_e}$ seem to be fundamental for the above behavior, we are going to prove that $\underline{\delta_e}$ is a saddle point bifurcation for the system (3.3). An analogous proof holds for $\overline{\delta_e}$.

Proposition 3.10. *The nonhyperbolic equilibrium at $\underline{\delta_e}$ is a saddle point bifurcation.*

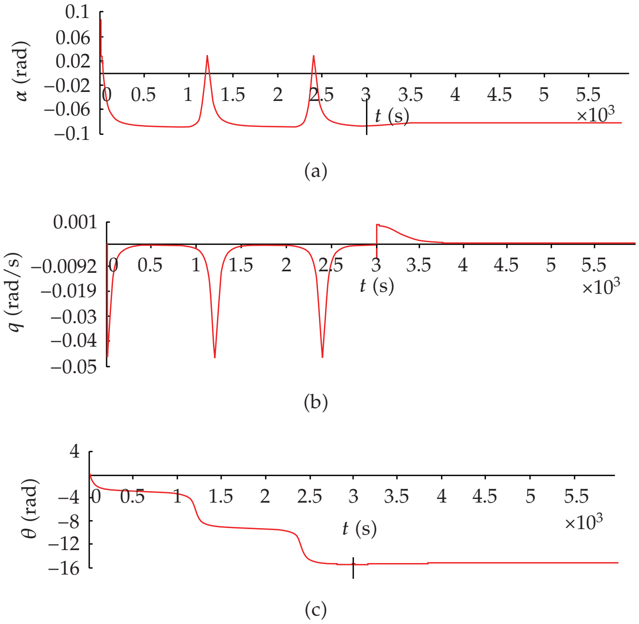

Figure 7: Resetting δ_e from $\delta_e'' = 0.048$ [rad] $= 2.751° < \underline{\delta_e}$ to $\delta_e' = -0.04678$ [rad] $= -2.681°$ after 3000 [s] of oscillations a stable equilibrium is recovered.

Proof. Let us pose $x = (\alpha, q, \theta)$ and write the system (3.3) as $\dot{x} = f(x, \delta_e)$. Moreover, set $\underline{Pe} = (\alpha_1(\underline{\delta_e}), 0, \theta_1(\underline{\delta_e})) = (\alpha_2(\underline{\delta_e}), 0, \theta_2(\underline{\delta_e}))$ the corresponding equilibrium point. As it has been already checked that $\underline{Pe}$ is a nonhyperbolic equilibrium point, it is sufficient to verify that $w \cdot D_{\delta_e} f \neq 0$ and $w \cdot D_x^2 f(v, v) \neq 0$, where v and w are right and left eigenvalues corresponding to the zero eigenvalues, respectively, and the derivatives are computed at $\underline{Pe}$, $\underline{\delta_e}$ [11, page 148]. From (3.3) it follows that $v = ((1/z_\alpha) \cdot (g/V) \cdot \sin\theta, 0, 1)^T$ and $w = (m_\alpha/(z_\alpha \cdot m_q - m_\alpha), -z_\alpha/(z_\alpha \cdot m_q - m_\alpha), 1)$ are right and left eigenvectors, respectively, corresponding to the zero eigenvalue and

$$w \cdot D_{\delta_e} f = \frac{m_\alpha \cdot z_{\delta_e} - z_\alpha \cdot m_{\delta_e}}{z_\alpha \cdot m_q - m_\alpha},$$

$$w \cdot D_x^2 f(v, v) = \frac{1}{z_\alpha \cdot m_q - m_\alpha} \cdot \left[-\frac{g}{V} \cdot \cos\theta \cdot m_\alpha + \frac{g}{V} \cdot \left(\overline{m_{\dot{\alpha}}} \cdot \cos\theta + \frac{c_2}{a} \cdot a_2 \cdot \sin\theta \right) \cdot z_\alpha \right]. \tag{3.9}$$

For the considered numerical data, given in Table 1, we have $w \cdot D_{\delta_e} f = -0.489 \neq 0$ and $w \cdot D_x^2 f(v, v) = 2.255 \neq 0$. Therefore, $\underline{Pe}$ is a saddle-node bifurcation. □

Remark 3.11. Along the path of longitudinal flight equilibriums only saddle-point bifurcation exists. There is no Hopf bifurcation.

Remark 3.12. In both cases, that is, decrease of the parameter δ_e under $\underline{\delta_e}$ or increase of the parameter δ_e over $\overline{\delta_e}$, we have a loss of steady state and occurrence of an oscillatory flight.

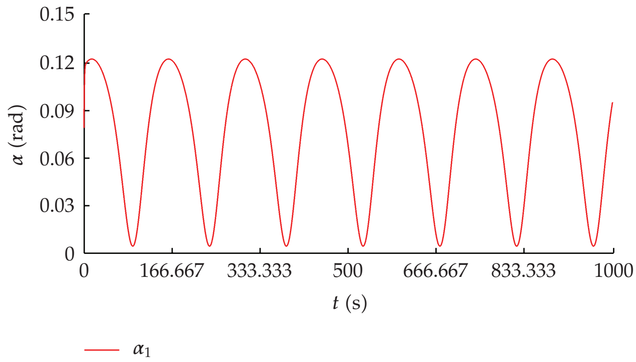

(a)

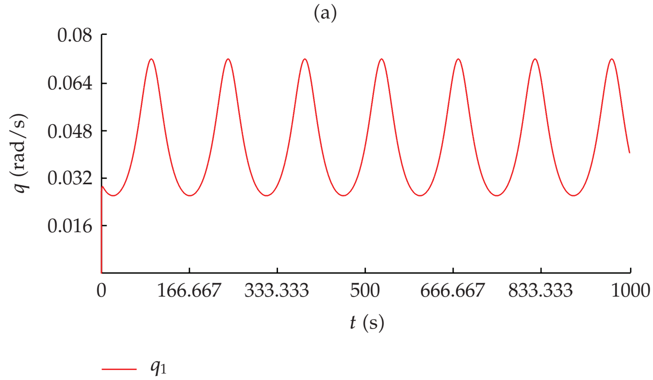

(b)

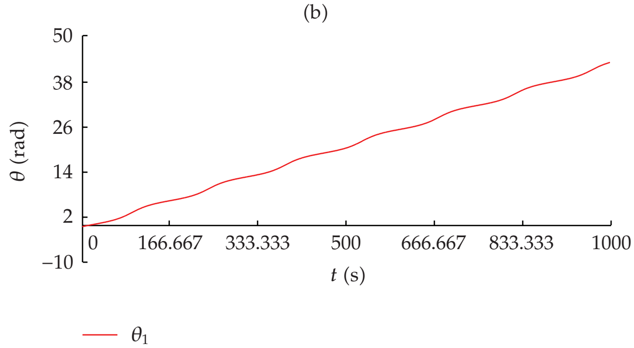

(c)

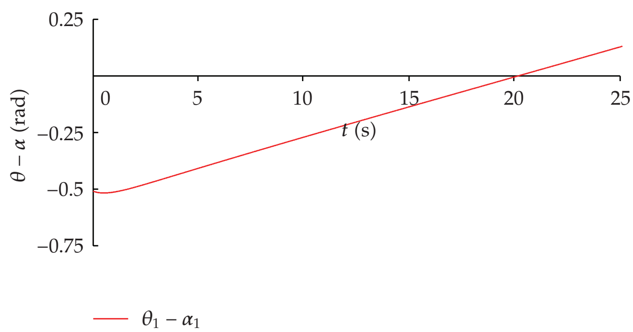

(d)

Figure 8: Transfer from $\alpha_1' = 0.0786697$ [rad] $= 4.509°$; $q_1' = 0$ [rad/s]; $\theta_1' = -0.428832$ [rad] $= -24.58°$ into a state which is appropriate for the touch-down moment: $\theta'' - \alpha'' = 0$ and $\theta'' > 0$ (θ'' small).

Computation shows that this loss is not catastrophic, because if δ_e is reset, then a stable equilibrium is recovered, as it is illustrated in Figure 7.

Remark 3.13. It is important to remark that the saddle-point bifurcation phenomenon occurring at $\underline{\delta_e}$ is of practical interest. Using this phenomenon it is possible to transfer the vehicle from a stable descending longitudinal flight equilibrium with constant forward velocity ($\theta < 0$ and $\theta - \alpha < 0$) into a state which is appropriate for the touch-down moment.

Definition 3.14. In a longitudinal flight with constant forward velocity an equilibrium is a descending flight if $\theta - \alpha < 0$.

Such an equilibrium is, for instance, $\alpha_1' = 0.078669740237840\,[\mathrm{rad}] = 4.509^\circ$; $q_1' = 0\,[\mathrm{rad/s}]$; $\theta_1' = -0.428832005303479\,[\mathrm{rad}] = -24.582^\circ$ and corresponds to $\delta_e' = -0.03866\,[\mathrm{rad}] = -2.216^\circ$. Moreover, it is stable descent flight equilibrium. By the maneuver $\delta_e' \to \delta_e''$ with $\delta_e'' = -0.1\,[\mathrm{rad}] = 5.732^\circ < \underline{\delta_e}$ the above state is transferred into a state which is appropriate for the touch-down moment $\theta'' - \alpha'' = 0$ and $\theta'' > 0$ (θ'' small) (Figure 8).

Figure 8 shows that the maneuver $\delta_e' = -0.03866\,[\mathrm{rad}] = -2.216^\circ \to \delta_e'' = -0.1\,[\mathrm{rad}] = -5.13^\circ$ made 20.16 [s] before the touch-down moment, transfers the aircraft in 20.16 seconds from the stable descending flight equilibrium $\alpha_1' = 4.509^\circ$; $q_1' = 0$; $\theta_1' = -24.5^\circ$ into the state $\alpha_1'' = \theta_1'' = 6.94^\circ$, which is appropriate for the touch-down moment. This flare maneuver has to be made when the aircraft is at $H = 840$ [m] altitude.

Remark 3.15. It is important to underline that the transfer period t depends strongly on the initial value δ_e' and on the final value δ_e'' of the elevator deflection.

If δ_e' is fixed and δ_e'' decreases, then t decreases and $\alpha'' = \theta''$ increases.

For instance, when $\delta_e' = -0.03866\,[\mathrm{rad}] = -2.216^\circ$, we have

$$\begin{gathered}
\delta_e'' = -0.049\,[\mathrm{rad}] = -2.80^\circ, \qquad t = 239.72\,[\mathrm{s}], \qquad \alpha'' = \theta'' = 0.089\,[\mathrm{rad}] = 5.1^\circ, \\
\delta_e'' = -0.1\,[\mathrm{rad}] = -5.73^\circ, \qquad t = 20.15\,[\mathrm{s}], \qquad \alpha'' = \theta'' = 0.1211\,[\mathrm{rad}] = 6.94^\circ, \\
\delta_e'' = -0.2\,[\mathrm{rad}] = -11.46^\circ, \qquad t = 8.15\,[\mathrm{s}], \qquad \alpha'' = \theta'' = 0.184\,[\mathrm{rad}] = 10.5^\circ.
\end{gathered} \tag{3.10}$$

Moreover, if the time interval between the moment of the elevator deflection change (flare) and the real touch-down moment is larger than the above presented periods of transitions, then the touch-down moment could be catastrophic, due to the oscillations.

Conclusion

In the simplified model it can be shown numerically that there exists a range $[\underline{\delta_e}, \overline{\delta_e}]$ of the values of the elevator deflection δ_e such that to a value δ_e from $[\underline{\delta_e}, \overline{\delta_e}]$ a set of equilibriums corresponds. Some of these equilibriums are stable and some of them are unstable. If $\delta_e', \delta_e'' \in (\underline{\delta_e}, \overline{\delta_e})$ a change $\delta_e' \to \delta_e''$ of the elevator deflection δ_e transfers the vehicle into a stable equilibrium corresponding to δ_e''. If $\delta_e' \in (\underline{\delta_e}, \overline{\delta_e})$ and $\delta_e'' < \underline{\delta_e} - k$ or $\delta_e'' > \overline{\delta_e} + k$ with $k > 0$, then the change $\delta_e' \to \delta_e''$ of the elevator deflection leads to an oscillatory movement of the vehicle , which is noncatastrophic from mathematical point of view. This is due to a saddle node bifurcation and can be useful for preparing the touch-down. Hopf bifurcations are not present.

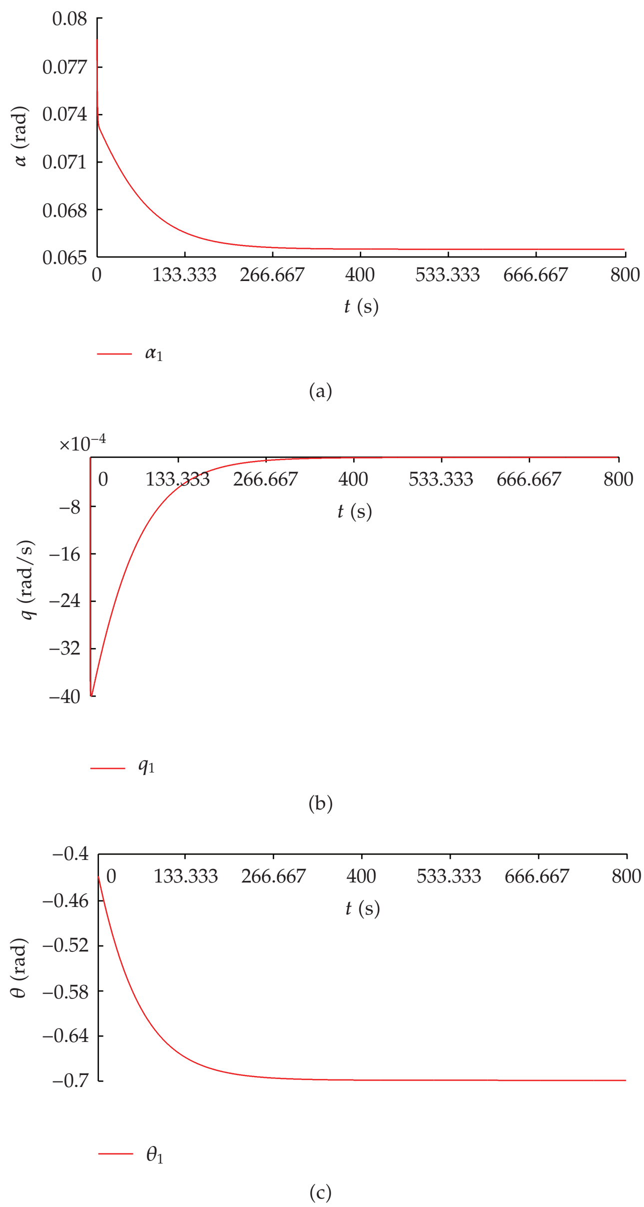

Figure 9: A transfer between two equilibriums, which belong to $\mathcal{D}_1$ (simulated in the general model): $\delta_e' = -0.03866\,[\text{rad}] = 2.216^\circ \rightarrow \delta_e'' = 0.03026\,[\text{rad}] = 1.734^\circ$. $\alpha_1' = 0.07866974\,[\text{rad}] = 4.509^\circ$; $q_1' = 0\,[\text{rad/s}]$; $\theta_1' = -0.428832\,[\text{rad}] = 24.582^\circ \rightarrow \alpha_1'' = 0.065516\,[\text{rad}] = 3.755^\circ$; $q_1'' = 0\,[\text{rad/s}]$; $\theta_1'' = -0.698066\,[\text{rad}] = -40.016^\circ$.

4. General Constant forward Velocity Longitudinal Flight Model of the ADMIRE Aircraft

Proposition 4.1. *The general constant forward velocity longitudinal flight model of the ADMIRE aircraft is defined by the system of differential equations:*

$$\begin{aligned}
\overset{\circ}{\alpha} &= q + \frac{g}{V} \cdot \cos(\theta - \alpha) - \frac{g}{V} \cdot \sin(\theta - \alpha) \cdot \tan\alpha + [z_\alpha \cdot \alpha + z_{\delta_e} \cdot \delta_e] \cdot \frac{1}{\cos\alpha}, \\
\overset{\circ}{q} &= m_\alpha \cdot \alpha + m_q \cdot q + \frac{g}{V} \cdot \left(\overline{m_{\overset{\circ}{\alpha}}} \cdot \cos\theta - \frac{c_2}{a} \cdot a_2 \cdot \sin\theta\right) + m_{\delta_e} \cdot \delta_e, \\
\overset{\circ}{\theta} &= q.
\end{aligned} \tag{4.1}$$

Proof. System (4.1) is obtained from the system (2.11), substituting the general aero dynamical forces and moments with those corresponding to the ADMIRE aircraft. □

Remark 4.2. The simplified model (3.3) is obtained from (4.1), approximating $\cos\alpha$ with 1 (small angle of attack $\alpha \approx 0$). If the simplified system (3.3) describes correctly the real phenomenon, then it has to be topologically equivalent to the system (4.1) [12]. Furthermore, the simplified system (3.3) has to be structurally stable. As far we know, the structural stability of the system (3.3) never was proved. What we intend to prove numerically in this paragraph is that the steady states (stable and unstable) of system (4.1) are exactly the same as those of system (3.3). Moreover, we show that the behavior of the aircraft described by (4.1) is similar to that described by (3.3). This is not a proof of the structural stability of the simplified system, but it is an increase of the believe that the simplified system (3.3) describes correctly the real phenomenon and we are not in the case reported in [13]. In [13] it was shown that the simplified system of differential equations which governs the motion of the automatic—landing flight—experiment (ALFLEX) reentry vehicle, is neither structurally stable, nor topologically equivalent to the general system governing the same motion. In other words, the general and the simplified mathematical models of ALFLEX give different images of the same reality.

Remark 4.3. According to the general nonlinear model, the equilibriums in a longitudinal flight with constant forward velocity $V$are solutions of the nonlinear system of equations:

$$\begin{aligned}
q + \frac{g}{V} \cdot \cos(\theta - \alpha) - \frac{g}{V} \cdot \sin(\theta - \alpha) \cdot \tan\alpha + [z_\alpha \cdot \alpha + z_{\delta_e} \cdot \delta_e] \cdot \frac{1}{\cos\alpha} &= 0, \\
m_\alpha \cdot \alpha + m_q \cdot q + \frac{g}{V} \cdot \left(\overline{m_{\overset{\circ}{\alpha}}} \cdot \cos\theta - \frac{c_2}{a} \cdot a_2 \cdot \sin\theta\right) + m_{\delta_e} \cdot \delta_e &= 0, \\
q &= 0.
\end{aligned} \tag{4.2}$$

System (4.2) defines the equilibrium manifold of the longitudinal flight with constant forward velocity V in the general model.

System (4.2) implies that α, θ satisfy

$$\begin{aligned}
\frac{g}{V} \cdot \cos(\theta - \alpha) - \frac{g}{V} \cdot \sin(\theta - \alpha) \cdot \tan\alpha + [z_\alpha \cdot \alpha + z_{\delta_e} \cdot \delta_e] \cdot \frac{1}{\cos\alpha} &= 0, \\
m_\alpha \cdot \alpha + \frac{g}{V} \cdot \left(\overline{m_{\overset{\circ}{\alpha}}} \cdot \cos\theta - \frac{c_2}{a} \cdot a_2 \cdot \sin\theta\right) + m_{\delta_e} \cdot \delta_e &= 0.
\end{aligned} \tag{4.3}$$

Since $(4.3)_1$ can be written in the form

$$\frac{1}{\cos\alpha}\cdot\left[\frac{g}{V}\cdot\cos\theta+z_\alpha\cdot\alpha+z_{\delta_e}\cdot\delta_e\right]=0, \tag{4.4}$$

the system (4.3) has the same solutions as the system

$$\begin{gathered}\frac{g}{V}\cdot\cos\theta+z_\alpha\cdot\alpha+z_{\delta_e}\cdot\delta_e=0,\\ m_\alpha\cdot\alpha+\frac{g}{V}\cdot\left(\overline{m_{\mathring{\alpha}}}\cdot\cos\theta-\frac{c_2}{a}\cdot a_2\cdot\sin\theta\right)+m_{\delta_e}\cdot\delta_e=0.\end{gathered} \tag{4.5}$$

It follows in this way.

Proposition 4.4. *In the case of the longitudinal flight with constant forward velocity of the ADMIRE aircraft the equilibrium manifold $\mathcal{M}_V$ in the general model is the same as in the simplified model.*

Proposition 4.5. *The eigenvalues of the linearized system at equilibrium are the solutions of the equation:*

$$-\lambda^3+\left(a_{11}+m_q\right)\cdot\lambda^2+\left(m_\alpha+a_{23}-a_{11}\cdot m_q\right)\cdot\lambda+m_\alpha\cdot a_{13}-a_{11}\cdot a_{23}=0, \tag{4.6}$$

where

$$\begin{aligned}a_{11}&=\frac{g}{V}\cdot\sin(\theta-\alpha)+\frac{g}{V}\cdot\cos(\theta-\alpha)\cdot\tan\alpha-\frac{g}{V}\cdot\sin(\theta-\alpha)\cdot\frac{1}{\cos^2\alpha}\\ &\quad+\frac{z_\alpha}{\cos\alpha}+\left[z_\alpha\cdot\alpha+z_{\delta_e}\cdot\delta_e\right]\cdot\frac{\sin\alpha}{\cos^2\alpha},\\ a_{13}&=-\frac{g}{V}\cdot\sin(\theta-\alpha)-\frac{g}{V}\cdot\cos(\theta-\alpha)\cdot\tan\alpha,\\ a_{23}&=\frac{g}{V}\cdot\left[-\overline{m_{\dot{\alpha}}}\cdot\sin\theta-\frac{c_2}{a}\cdot a_2\cdot\cos\theta\right]\end{aligned} \tag{4.7}$$

or

$$\begin{aligned}a_{11}&=\frac{z_\alpha}{\cos\alpha}+\frac{g}{V}\cdot\frac{\sin\theta}{\cos\alpha}-\frac{g}{V}\cdot\frac{\sin(\theta-\alpha)}{\cos^2\alpha}+\left[z_\alpha\cdot\alpha+z_{\delta_e}\cdot\delta_e\right]\cdot\frac{\sin\alpha}{\cos^2\alpha},\\ a_{13}&=-\frac{g}{V}\cdot\frac{\sin\theta}{\cos\alpha},\\ a_{23}&=-\frac{g}{V}\cdot\left[\overline{m_{\mathring{\alpha}}}\cdot\sin\theta+\frac{c_2}{a}\cdot a_2\cdot\cos\theta\right]\end{aligned} \tag{4.8}$$

and α, q, and θ are the coordinates of the equilibrium.

Proof. The proof is given by computation. □

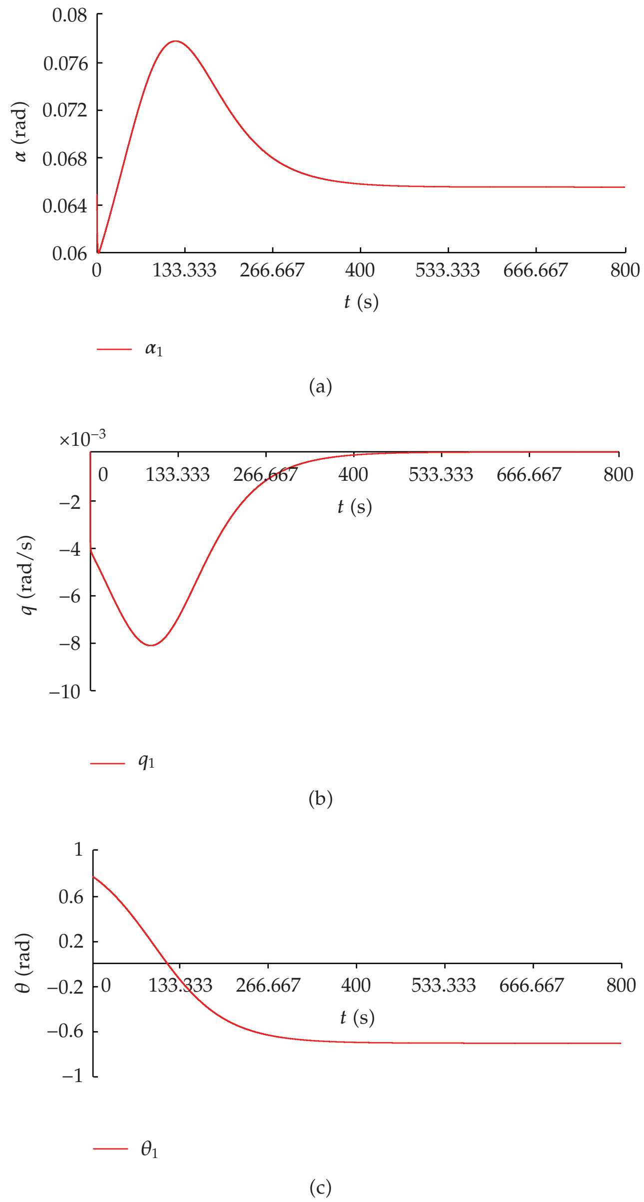

Figure 10: A transfer of an equilibrium, which belongs to $\wp_2$, into an equilibrium which belongs to $\wp_1$ (simulated in the general model): $\delta_e' = -0.03866\,[\text{rad}] = 2.216^\circ \rightarrow \delta_e'' = 0.03026\,[\text{rad}] = 1.734^\circ$. $\alpha_2' = 0.064883\,[\text{rad}] = 3.719^\circ$; $q_2' = 0\,[\text{rad/s}]$; $\theta_2' = 0.7674624\,[\text{rad}] = 43.994^\circ \rightarrow \alpha_1'' = 0.065516\,[\text{rad}] = 3.755^\circ$; $q_1'' = 0\,[\text{rad/s}]$; $\theta_1'' = -0.6980667\,[\text{rad}] = -40.016^\circ$ instead of $\alpha_2' = 0.064883\,[\text{rad}] = 3.719^\circ$; $q_2' = 0\,[\text{rad/s}]$; $\theta_2' = 0.7674624\,[\text{rad}] = 43.994^\circ \rightarrow \alpha_2'' = 0.046845\,[\text{rad}] = 2.685^\circ$; $q_2'' = 0\,[\text{rad/s}]$; $\theta_2'' = 1.03669718\,[\text{rad}] = 59.428^\circ$.

Table 2: The transfer periods of the transitions corresponding to the maneuver $\delta_e' = -0.03866\,[\text{rad}] = -2.216^\circ \rightarrow \delta_e''$.

δ_e'' [rad]	−0.048	−0.05	−0.06	−0.08	−0.1	−0.5
Transfer period [s]	333	170	70	30	20	4

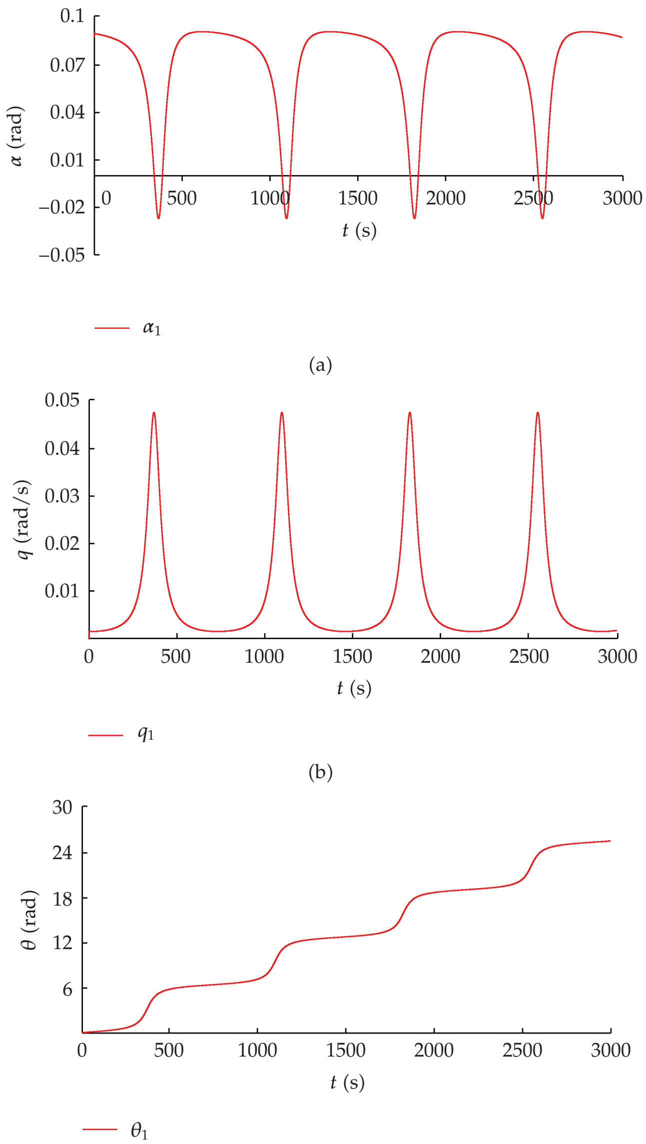

(a)

(b)

(c)

Figure 11: Oscillations when $\delta_e' = -0.04678$ [rad] $= -2.681°$ $\rightarrow$ $\delta_e'' = -0.05$ [rad] $= -2.866°$ and the starting point is $\alpha_1' = 0.0869742$ [rad] $= 4.985°$; $q_1' = 0$ [rad/sec]; $\theta_1' = 0.159329$ [rad] $= 9.133°$.

Remark 4.6. Computing the roots of (4.6) at the equilibriums of $\mathcal{P}_1$ we find that these are negative real numbers for $\delta_e \in (\underline{\delta_e}, \overline{\delta_e})$, and for $\delta_e = \underline{\delta_e}$ or $\delta_e = \overline{\delta_e}$ one of the roots is equal to zero.

Computing the roots of (4.6) at the equilibriums of $\mathcal{P}_2$ we find that two of them are negative real numbers and one is strictly positive for $\delta_e \in (\underline{\delta_e}, \overline{\delta_e})$, and for $\delta_e = \underline{\delta_e}$ or $\delta_e = \overline{\delta_e}$ one of the roots is equal to zero.

We conclude the following.

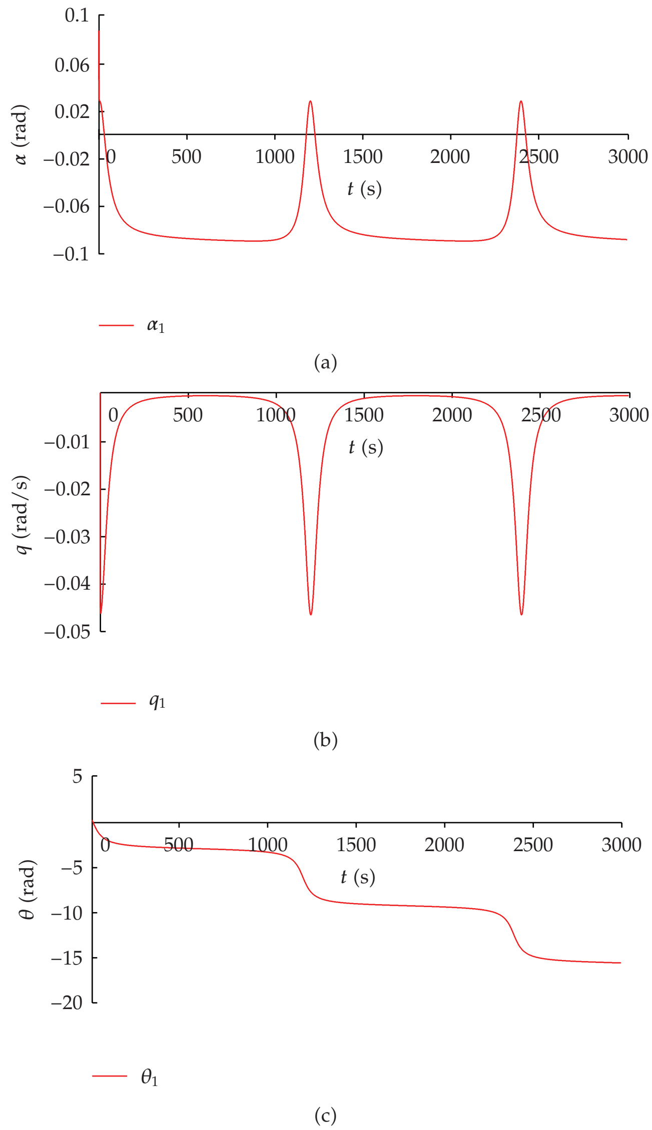

Figure 12: Oscillations when $\delta_e' = -0.04678$ [rad] $= -2.681°$ $\rightarrow$ $\delta_e'' = -0.05$ [rad] $= -2.866°$ and the starting point is $\alpha_1' = 0.086974288$ [rad] $= 4.985°$; $q_1' = 0$ [rad/sec]; $\theta_1' = 0.1593297$ [rad] $= 9.133°$.

Proposition 4.7. *An equilibrium is stable in the general model if and only if it is stable in the simplified model. Moreover,* $\underline{\delta_e}$, $\overline{\delta_e}$ *are saddle-points in both models.*

Remark 4.8. The same transfer maneuver between the same equilibriums which belong to a conex part of $\mathcal{P}_1 = \{(\alpha_1(\delta_e), 0, \theta_1(\delta_e)) : \delta_e \in (\underline{\delta_e}, \overline{\delta_e})\}$, simulated already in simplified model, is simulated now in the framework of the general model in Figure 9.

The same transfer maneuver from an unstable equilibrium which belongs to $\mathcal{P}_2 = \{(\alpha_2(\delta_e), 0, \theta_2(\delta_e)) : \delta_e \in (\underline{\delta_e}, \overline{\delta_e})\}$ into a stable equilibrium which belongs to $\mathcal{P}_1$, simulated

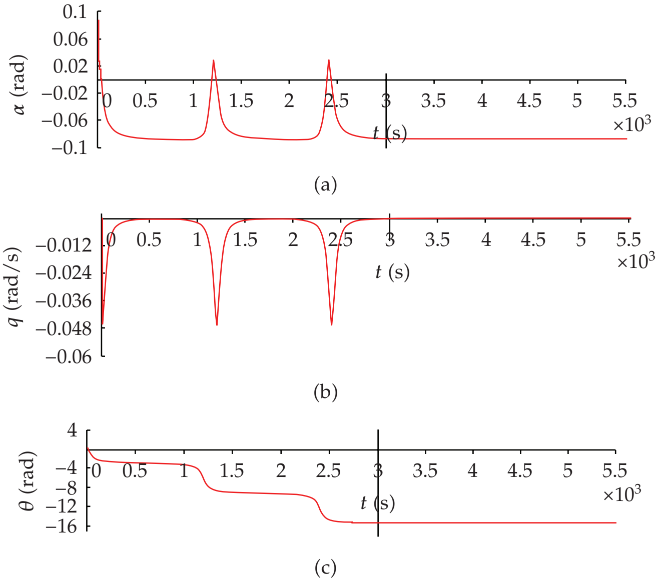

Figure 13: Resetting δ_e from $\delta_e'' = 0.048$ [rad] $= 2.751° < \underline{\delta_e}$ to $\delta_e' = -0.04678$ [rad] $= -2.681°$ after 3000 [s] of oscillations a stable equilibrium is recovered.

already in simplified model, is simulated now in the framework of the general model in Figure 10.

Remark 4.9. The above simulations show that from the point of view of this type of transfer, the results obtained in general model are similar to those obtained in the simplified model. More about transfer maneuvers can be found in [14].

Remark 4.10. The behavior of the ADMIRE aircraft, when the maneuver $\delta_e' \to \delta_e''$ is so that $\delta_e' \in (\underline{\delta_e}, \overline{\delta_e})$ and $\delta_e'' \notin (\underline{\delta_e}, \overline{\delta_e})$, simulated in general model, is represented in Figures 11 and 12 and shows that this is similar to that obtained in the simplified model.

Remark 4.11. Moreover, the simulation in general model shows that the loss of stability, due to maneuver, is noncatastrophic (from mathematical point of view), because if δ_e is reset, then a stable equilibrium is recovered; see Figure 13.

Remark 4.12. The bifurcation phenomenon at $\underline{\delta_e}$, present also in the general model, can be used for the transfer of the aircraft from a stable descending longitudinal flight equilibrium into a state which is appropriate for the touch-down moment. The simulation of such a transfer is presented in Figure 14.

Remark 4.13. The flare maneuver has to be made also when the aircraft is at 840 [m] altitude, but the transfer period, computed in the general model can be different, as it is shown in Table 2.

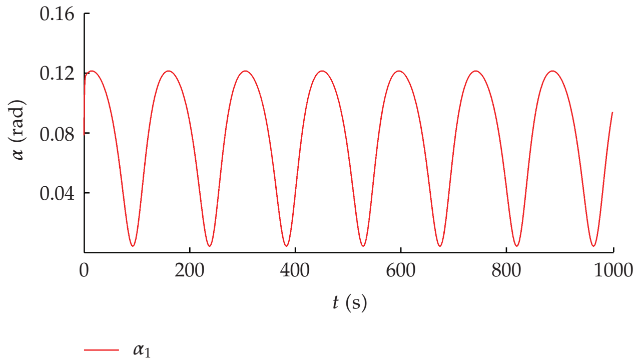

(a)

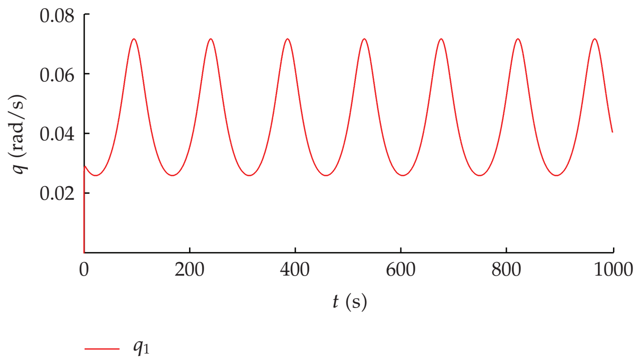

(b)

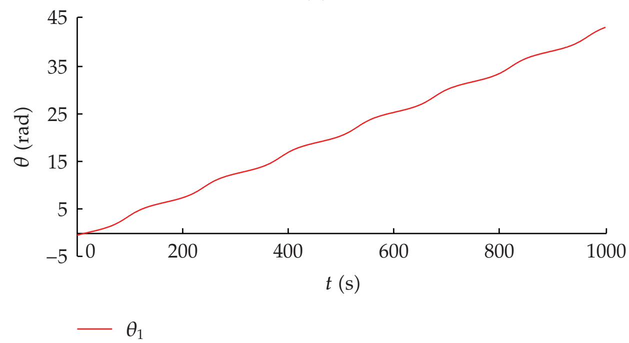

(c)

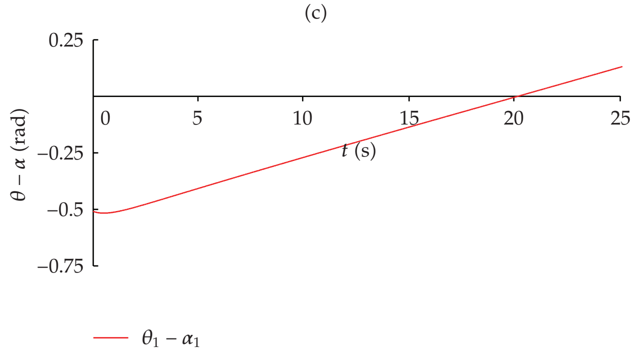

(d)

Figure 14: Transfer from $\alpha_1' = 0.0786697$ [rad] $= 4.509°$; $q_1' = 0$ [rad/s]; $\theta_1' = -0.428832$ [rad] $= -24.58°$ into a state which is appropriate for the touch-down moment $\theta'' - \alpha'' = 0$ and $\theta'' > 0$ (θ'' small).

5. Conclusions

(i) Numerical computation shows that there exists a range $[\underline{\delta_e}, \overline{\delta_e}]$ of the elevator deflection values δ_e, such that to a value δ_e from $[\underline{\delta_e}, \overline{\delta_e}]$ the same set of equilibriums corresponds in both models.

(ii) An equilibrium is stable in the simplified model if and only if it is stable also in the general model.

(iii) If $\delta_e', \delta_e'' \in [\underline{\delta_e}, \overline{\delta_e}]$, a change $\delta_e' \to \delta_e''$ of the elevator deflection δ_e transfers the vehicle into a stable equilibrium corresponding to δ_e'' in both models.

(iv) If $\delta_e' \in [\underline{\delta_e}, \overline{\delta_e}]$ and $\delta_e'' < \delta_e - k$ or $\delta_e'' > \overline{\delta_e} + k$ with $k > 0$, then the change $\delta_e' \to \delta_e''$ of the elevator deflection leads to a noncatastrophic oscillatory movement of the vehicle, in both models. This is due to the saddle node bifurcation in both models and can be used for preparing the touch-down in both models.

(v) In both models there is no Hopf bifurcation.

(vi) The similarity of the computed results increases the confidence that the simplified model correctly describes the real longitudinal flight, but it is not a proof of the structural stability of the simplified model. Such a proof would be welcome.

Acknowledgments

The authors thank the anonymous referees for their valuable comments, which led to the improvement of the manuscript. St. Balint and A. M. Balint thank the Romanian National Authority for Research for supporting the research under the Grant ID 354 no.7/2007.

References

[1] R. K. Mehra and R. K. Prasanth, "Bifurcation and limit cycle analysis of nonlinear pilot induced oscillations," in *Proceedings of the AIAA Atmospheric Flight Mechanics Conference and Exhibit*, Boston, Mass, USA, August 1998, AIAA-1998-4249.

[2] *Unified Pilot-Induced Oscillation Theory*, vol. 1–4, Wright-Patterson AFB, Ohio, 1996, WL-TR-96.

[3] B. A. Kish, et al., "A limited flight test investigation of pilot-induced oscillation due to rate limiting," in *Proceedings of the AIAA Guidance, Navigation, and Control Conference*, New Orleans, La, USA, August 1997, AIAA Paper 97-3703.

[4] D. H. Klyde, D. T. McRuer, and T. T. Myers, "Pilot-induced oscillation analysis and prediction with actuator rate limiting," *Journal of Guidance, Control, and Dynamics*, vol. 20, no. 1, pp. 81–89, 1997.

[5] R. K. Mehra, et al., "Global stability and control analysis of aircraft at high angles of attack," Tech. Rep. ONR-CR215-248, 1977.

[6] A. Ionita and A. Halanay, "Delay induced oscillations," in *Proceedings of the AIAA Atmospheric Flight Mechanics Conference*, New Orleans, La, USA, August 1997, AIAA-97-3502.

[7] J. S. Shamma and M. Athans, "Guaranteed properties of gain scheduled control for linear parameter-varying plants," *Automatica*, vol. 27, no. 3, pp. 559–564, 1991.

[8] B. Etkin and L. Reid, *Dynamics of Flight: Stability and Control*, John Wiley & Sons, New York, NY, USA, 1996.

[9] M. Cook, *Flight Dynamics Principles*, John Wiley & Sons, New York, NY, USA, 1997.

[10] St. Balint, A. M. Balint, and A. Ionita, *Journal of Aerospace Engineering*. In press.

[11] J. Guckenheimer and P. Holmes, *Nonlinear Oscillations, Dynamical Systems, and Bifurcations of Vector Fields*, vol. 42 of *Applied Mathematical Sciences*, Springer, New York, NY, USA, 1983.

[12] Y. A. Kuznetsov, *Elements of Applied Bifurcation Theory*, vol. 112 of *Applied Mathematical Sciences*, Springer, New York, NY, USA, 2nd edition, 1998.

[13] E. Kaslik and S. Balint, "Structural stability of simplified dynamical system governing motion of ALFLEX reentry vehicle," *Journal of Aerospace Engineering*, vol. 20, no. 4, pp. 215–219, 2007.

[14] Ş. Balint, L. Brăescu, and E. Kaslik, *Regions of Attraction and Applications to Control Theory*, vol. 1 of *Mathematical Problems in Engineering and Aerospace Sciences*, Cambridge Scientific, Cambridge, UK, 2008.